Organometallics **1988,** *7,* 2575-2577 2575

lacycle has a butterfly angle of 144.7°, and the C–M–C bond angle is 93.4 (3)°. The Co–C(1) and Co–C(13) bond distances are 1.985 (6) and 1.959 (7) Å, respectively. Again, the methylene carbon has a large central ring bond angle of 115.2 (6)°. Selected bond angles and distances for **1** and **3** are provided in the captions of the figures.

The transition-metal molecular orbitals involved in bonding with Cp_2MR_2 complexes have been outlined by Hoffmann and co-workers.[12] Folding of the metallacycle (the angle ω in our metallacycle **1** is 19.9°, Figure 3) would be necessary for π overlap of the Cp_2M vacant Frontier $1a_1$ orbital (Figure 3) with the HOMO of the organic ligand. Such overlap could enhance the observed nonplanar conformation and shorten the Ti–C(1) and Ti–C(13) bond distances in **1**. The crystal structures of **1** exhibits a boat conformation for the central ring where the methylene hydrogens are nonequivalent. In order to ascertain the relative boat vs planar conformational energies and hence the contribution of the $1a_1$–HOMO π overlap in **1** and **2**, we turned to variable-temperature NMR studies. In the ^1H NMR spectrum (25 °C, THF-d_8, 90 MHz) of **1**, the methylene hydrogens appear as a singlet at δ 3.91 ppm, indicative of a fast-exchange boat–boat interconversion process (Figure 4). At –50 °C, broadening was observed for the methylene hydrogen resonance; however, coalescence was not achieved with temperatures as low as –75 °C. Similar experiments were performed on our hafnacycle **2** (CD_2Cl_2/CF_2Br_2, 1:3, as solvent). Again, the methylene hydrogen resonance broadened, but coalescence was not obtained. These experiments suggest a low $\Delta G^{\ddagger}$ for boat–boat interconversion in **1** and **2**. Furthermore, if π overlap plays a role in conformational stability (and concomitant shortening of the Ti–C bonds in **1**), its contribution to the energy stabilization of the boat conformation is minimal.[13] Finally, in the case of cobaltacycle **3**, its methylene protons give an AB spectrum at room temperature (H_A, δ 4.22 ppm, H_B, δ 3.95 ppm, J_{AB} = 15.8 Hz) consistent with a nonfluxional thermodynamically more stable boat structure (ω = 27.9° in the crystal structure) where the bulky triphenylphosphine ligand occupies an equatorial position (Figure 4A).[13]

Further work concerning the preparation, conformational analysis, and chemistry of metallacyclohexa-2,5-dienes is being pursued.

Acknowledgment. We thank Dr. J. Lay, Jr., at the National Center for Toxicological Research for the high-resolution mass spectral data. We would also like to thank the National Science Foundation (CHE-8312644) and the donors of the Petroleum Research Fund, administered by the American Chemical Society, for partial funding of this research.

Supplementary Material Available: Tables of crystallographic data collection and refinement details, atomic coordinates and equivalent isotropic thermal parameters, distances and angles in $C_{13}H_{10}Ti(cpd)_2$ and $C_{13}H_{10}Co(cpd)(PPh_3)$, and anisotropic thermal parameters (13 pages); listings of structure factor amplitudes for $C_{13}H_{10}Ti(cpd)_2$ and $C_{13}H_{10}Co(cpd)(PPh_3)$ (37 pages). Ordering information is given on any current masthead page.

---

(12) (a) Lauher, J. W.; Hoffmann, R. *J. Am. Chem. Soc.* **1976**, *98*, 1729–1742. See also: Tatsumi, K.; Nakamura, A.; Hofmann, P.; Stauffert, P.; Hoffmann, R., *J. Am. Chem. Soc.* **1985**, *107*, 4440–4451. (b) Thorn, D. L.; Hoffman, R., Nouv. *J. Chim.* **1979**, *3*, 39–45.

(13) MMX minimization of **1**, **2**, and **3** also gave boat conformations (ω = 25° and 17° for **1** and **2**, respectively). Further calculations performed for simulation of the boat–boat interconversion of **1** and **2** gave barriers of 0.68 and 1.13 kcal/mol, respectively. Such calculations take into account steric and torsional contributions of the ligands with the metal torsional effects being negligible. The energy differences determined by MMX calculations between boat forms of **3** (parts A and B of Figure 4 with ω = 33°) was 21 kcal/mol in favor of the equatorial PPh_3 conformation. Cf. Bowen, J. P.; Pathiaseril, A.; Profeta, S., Jr.; Allinger, N. L. *J. Org. Chem.* **1987**, *52*, 5162 and references cited. PC Model/MMX molecular modeling program: Serena Software, Box 3076, Bloomington, IN 47402-3076.

(14) King, R. B. *Inorg. Chem.* **1966**, *5*, 82–87.

Redox-Induced Reversible Migration of Hydrogen from Metal to Alkene

Claudio Bianchini,*,[†] Franco Laschi,[‡] Andrea Meli,[†] Maurizio Peruzzini,[†] Piero Zanello,[‡] and Piero Frediani[§]

Istituto per lo Studio della Stereochimica ed
Energetica dei Composti di Coordinazione
C N R Via J. Nardi 39, 50132 Firenze, Italy
Dipartimento di Chimica, Università di Siena
53100 Siena, Italy, and
Dipartimento di Chimica Organica, Università di Firenze
50121 Firenze, Italy

Received September 13, 1988

Summary: Reaction of the trihydride (triphos)RhH_3 (**1**) [triphos = $MeC(CH_2PPh_2)_3$] in benzene with dimethyl acetylenedicarboxylate (DMAD) (room temperature) or with excess dimethyl fumarate (DMFU) (reflux temperature) gives (triphos)RhH(π-DMFU) (**2**). Two-electron chemical or electrochemical oxidation of **2** in THF promotes hydride migration on the alkene. As a result, the succinyl complex $[(triphos)Rh\{CH(COOMe)CH_2(COOMe)\}]^{2+}$ forms, which can be isolated as an $SO_3CF_3^-$ (**3**) or ClO_4^- (**3a**) salt. One-electron reduction of **3** (or **3a**) in CH_2Cl_2 by macroelectrolysis at controlled potential permits one to obtain the square-pyramidal Rh(II) $[(triphos)Rh\{CH(COOMe)CH_2(COOMe)\}]^+$ (**4**), which has been characterized by ESR spectroscopy. Addition of one electron to **4** or two electrons to **3** (or **3a**) yields the starting hydride (fumarate) complex **2**.

The formal insertion of olefins into metal–hydrogen bonds and the microscopic reverse process, β-H elimination, are fundamental transformations in organometallic chemistry. Much is known about the kinetics and mechanism of these reactions; in particular, it is agreed that externally added ligands may promote the insertion and stabilize the alkyl complex with no variation of the formal oxidation state of the metal.[1] We now wish to report an example of hydride (alkene) → alkyl interconversion which is strictly controlled by the oxidation state of the metal.

The trihydride $[(triphos)RhH_3]^2$ (**1**) [triphos = $MeC(CH_2PPh_2)_3$] reacts in benzene with dimethyl acetylenedicarboxylate (DMAD) at room temperature or with excess dimethyl fumarate (DMFU) at reflux temperature yielding pale yellow crystals of $[(triphos)RhH(\pi\text{-DMFU})]^3$ (**2**) (yield 95%). The reaction with DMFU is accompanied by production of dimethyl succinate (DMSU) due to hydrogenation of excess olefin (Scheme I). Two-electron oxidation of the cis hydride (alkene) complex **2** in THF by chemical (2 equiv of $AgSO_3CF_3$) or electrochemical (ex-

---

[†] ISSECC, CNR.

[‡] University of Siena

[§] University of Firenze.

0276-7333/88/2307-2575$01.50/0

Scheme I

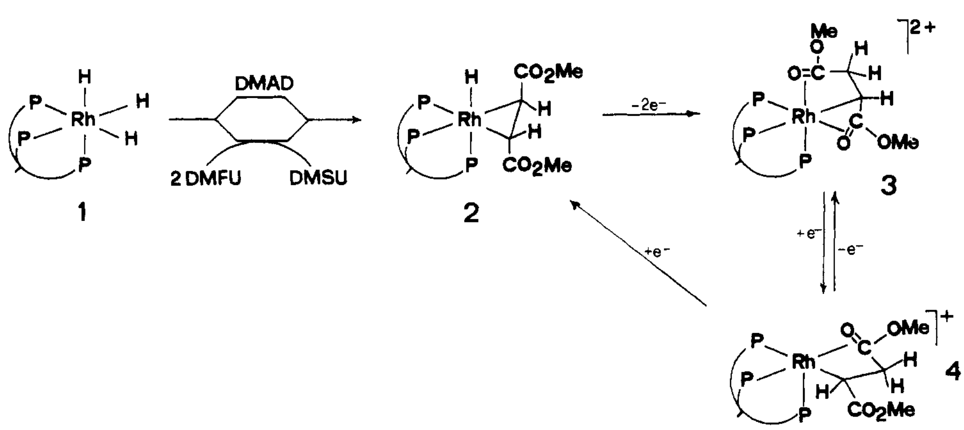

haustive electrolysis at +1.0 V, $[NBu_4]ClO_4$, 0.1 mol dm^{-3}) methods results in the formation of white needles of the succinyl complexes $[(triphos)Rh\{CH(COOMe)CH_2(COOMe)\}](SO_3CF_3)_2$ (**3**) and $[(triphos)Rh\{CH(COOMe)CH_2(COOMe)\}](ClO_4)_2$ (**3a**), respectively (yield 95%).[4] Compounds **3** and **3a** are reconverted into **2** either by reduction in THF with 2 equiv of $NaC_{10}H_8$ or by macroelectrolysis in CH_2Cl_2 at −1.0 V. Figure 1a illustrates the cyclic voltammetric response exhibited by **2** in THF. This complex undergoes a two-electron anodic process at peak A (E_p = +0.52 V), generating a product which reduces in two distinct steps (peaks B and C). This oxidation product **3a** is poorly soluble in THF; however its cyclic voltammetric fingerprint in CH_2Cl_2 (Figure 1b) is fully coincident with that of the product obtained by chemical oxidation of **2**. In fact, **3a** undergoes a first uncomplicated reduction process ($E^{\circ\prime}$ = −0.14 V), followed by an irreversible second step (E_p = −0.70 V). The anodic peak at E_p = +0.42 V, which is present in the reverse scan after traversing the most cathodic reduction step (this value coincides with the peak potential value for the oxidation of **2** in CH_2Cl_2), suggests that an exhaustive cathodic reduction at the potential of the second process should regenerate **2**. In actuality, electrolysis of a suspension of **3** (or **3a**) in THF at −1.0 V consumes 2 e/molecule and gives **2**. The product corresponding to the first cathodic process (i.e. after the consumption of 1e/molecule of **3** or **3a**) has been electronically and structurally characterized by ESR spectroscopy in solution as the Rh(II), square-pyramidal complex $[(triphos)Rh\{CH(COOMe)CH_2(COOMe)\}]^+$ (**4**). The frozen and room-temperature X-band ESR spectra in CH_2Cl_2 of the electrogenerated species are shown in Figure 2. Both spectra can be interpreted by using a $S = {}^1/_2$ spin Hamiltonian. The pattern $g_\perp$ (2.108) > $g_\parallel$ (2.002) ≅ 2.000 and the large $A_\perp$ (226.7 G) and $A_\parallel$ (272.0 G) values indicate that the complex in CH_2Cl_2 glass at 100 K exhibits a square-pyramidal geometry with the unpaired electron strongly coupled to the apical phosphorus.[5,6] A

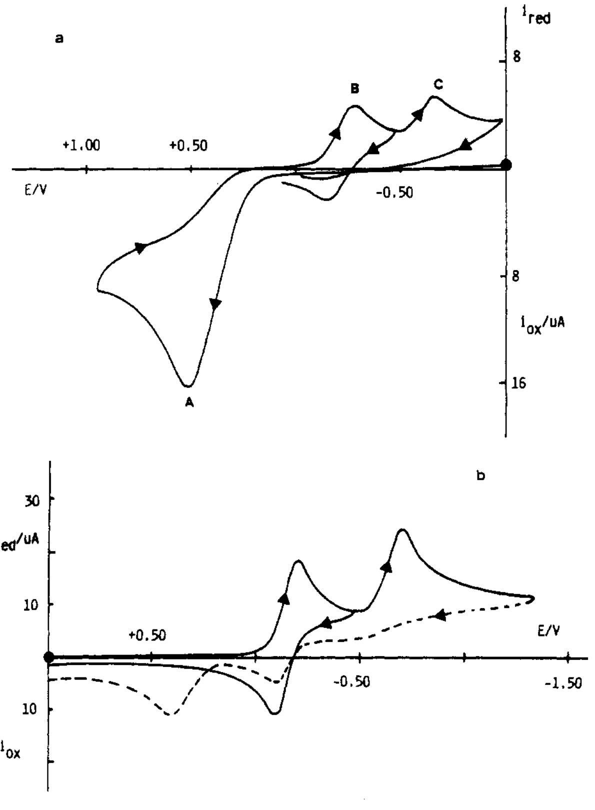

Figure 1. Cyclic voltammogram responses recorded at a platinum electrode under the following experimental conditions: (a) THF solution containing **2** (9.6×10^{-4} mol dm^{-3}) and $[NBu_4]ClO_4$ (0.1 mol dm^{-3}); (b) CH_2Cl_2 solution containing **3a** (1.40×10^{-3} mol dm^{-3}) and $[NBu_4]ClO_4$ (0.1 mol dm^{-3}) (scan rate = 0.2 V s^{-1}).

---

(1) (a) Doherty, N. M.; Bercaw, J. E. *J. Am. Chem. Soc.* **1985**, *107*, 2670 and ref. therein. (b) Schmidt, G. F.; Brookhart, M. *ibid.* **1985**, *107*, 1443.

(2) Ott, J.; Venanzi, L. M.; Ghilardi, C. A.; Midollini, S.; Orlandini, A. *J. Organomet. Chem.* **1985**, *291*, 89.

(3) Anal. Calcd (Found): C, 64.68 (64.50); H, 5.54 (5.62), Rh, 11.79 (11.67). IR (Nujol): 1690 (s), 1680 (s) cm^{-1} (free C═O). $^{31}P\{^1H\}$ NMR (C_6D_6, 121.42 MHz, 85% H_3PO_4, 298 K): AMQX spin system, $\delta(P_A)$ 4.57 ppm, $\delta(P_M)$ 23.04 ppm, $\delta(P_Q)$ 23.34 ppm, $J(P_AP_M)$ = 30.04, $J(P_AP_Q)$ = 29.74, $J(P_ARh)$ = 80.67, $J(P_MP_Q) \cong 2$, $J(P_MRh)$ = 130.65, $J(P_QRh)$ = 132.65 Hz. ^1H NMR (CD_2Cl_2, 300 MHz, TMS, 298 K): CH–CH, ABX-$P_AP_MP_Q$ spin system, $\delta(H_A)$ 4.55 (1 H), $\delta(H_B)$ 3.75 (1 H), $J(H_AH_B)$ = 8.84, $J(H_ARh)$ = 9.12, $J(H_BRh)$ = 8.55, $J(H_BP_A)$ = 8.55, $J(H_AP_A)$ = 4.82, $J(H_BP_M)$ = 1.20, $J(H_BP_Q)$ = 1.20, $J(H_AP_M)$ = 2.31, $J(H_AP_Q)$ = 2.31 Hz; OCH_3, s, δ 3.32 (3 H), 3.52 (3 H); Rh–H, $HXP_AP_MP_Q$ spin system, δ −11.72, $J(HRh)$ = 8.01, $J(HP_A)$ = 181,24, $J(HP_M)$ = 4.87, $J(HP_Q) \cong 2$ Hz. ^{13}C NMR ($CDCl_3$, 75.429 MHz, 298 K): $COOCH_3$ 179.82, 178.24 ppm; PC_6H_5 136–128 ppm; OCH_3 52.37, 51.90 ppm; C═C 67.99 ppm; CH_3 38.20 ppm; C 37.50 ppm; CH_2 37–32 ppm.

(4) Anal. Calcd for **3** (Found): C, 50.26 (50.17); H, 4.13 (4.08); Rh, 8.79 (8.82). Calcd for **3a** (Found): C, 52.68 (52.57); H, 4.51 (4.56); Rh, 9.60 (9.52); Cl, 6.61 (6.71). IR (Nujol): 1620 (s), 1580 (s) cm^{-1} (coordinated C═O). $^{31}P\{^1H\}$ NMR (CD_2Cl_2, 121.42 MHz, 298 K): AMQX pattern, $\delta(P_A)$ − 10.51 ppm, $\delta(P_M)$ 21.48 ppm, $\delta(P_Q)$ 37.12 ppm, $J(P_AP_M)$ = 32.79, $J(P_AP_Q)$ = 23.28, $J(P_ARh)$ = 79.10, $J(P_MP_Q)$ = 37.35, $J(P_MRh)$ = 120.62, $J(P_QRh)$ = 132.17 Hz. ^1H NMR (CD_2Cl_2, 300 MHz, TMS, 298 K): OCH_3, s, δ 3.41 (3 H), 4.26 (3 H); CH–CH_2, m, δ 3.20 (1 H), 2.30 (2 H). ^{13}C NMR ($CDCl_3$, 75.429 MHz, 298 K): $COOCH_3$ 195.20, 193.70 ppm; PC_6H_5 136–128 ppm; OCH_3 49.42, 48.90 ppm; CH_3 38.20 ppm; C 37.50 ppm; PCH_2 and CH–CH_2 37–30 ppm; Rh–CH 17.60 ppm, $^1J(RhC)$ = 14 Hz. Thermal decomposition at 250 °C produces DMSU.

(5) Bencini, A.; Gatteschi, D. *Transition Met. Chem.* (*N.Y.*) **1982**, *8*, 1.

(6) (a) Bianchini, C.; Laschi, F.; Ottaviani, F.; Peruzzini, M.; Zanello, P. *Organometallics* **1988**, *7*, 1660. (b) Bianchini, C.; Masi, D.; Mealli, C.; Meli, A.; Sabat, M.; Vizza, F. *Inorg. Chem.*, in press.

Figure 2. X-Band ESR spectra of $[(\mathrm{triphos})\mathrm{Rh}\{\mathrm{CH(COOMe)CH_2(COOMe)}\}]^+$ in CH_2Cl_2 at 100 K (a) and at 298 K (b).

three-line resolution in each perpendicular absorption is assigned to interaction with the basal phosphorus atoms ($A \cong 18$ G). The spectrum at 298 K consists of a doublet of doublets with $\langle g \rangle = 2.070$ ($\langle g_{\mathrm{calcd}} \rangle = 2.072$). The large value of $\langle A_{\mathrm{P_{apical}}} \rangle$ (234.7 G) is still present whereas the apparent coupling to only one basal phosphorus ($\langle A \rangle = 18$ G) is consistent with a remarkable distortion in the coordination polyhedron.[6]

One-electron reduction of the Rh(II) succinyl restores the starting cis hydride (alkene) 2. Reasonably, a Rh(I) succinyl complex forms which transforms to 2 via β-H elimination as soon as generated at the electrode surface.

In the attempt of understanding why oxidation of 2 induces olefin insertion, the following additional experimental pieces of information are noteworthy. (i) The related cis hydride(ethylene) complex $[(\mathrm{triphos})\mathrm{RhH(C_2H_4)}]$[7] (5) undergoes ethylene insertion across the Rh–H bond by reaction with either excess ethylene to form $[(\mathrm{triphos})\mathrm{Rh(C_2H_5)(C_2H_4)}]$[7] or 1 atm of CO to give $[(\mathrm{triphos})\mathrm{Rh(C_2H_5)(CO)}]$.[7] In contrast, ethylene insertion is not promoted by chemical or electrochemical oxidation. (ii) Compound 2 in THF solution is stable when treated with excess DMFU, ethylene, or CO even at reflux temperature. On the other hand, 2 (THF, room temperature) proves an efficient catalyst for the isomerization of the cis olefin dimethyl maleate (DMMA) to the trans isomer DMFU, thus indicating the occurrence of olefin insertion/β-H elimination. In the light of these results, it is evident that the CO_2Me substituents on the alkene play a key role in promoting the hydride (DMFU) → succinyl conversion. In particular, the ester C═O groups can electronically and coordinatively saturate rhodium during the oxidation process. Obviously, this is most important to stabilize both the dicationic (3 or 3a) and monocationic (4) species.

Registry No. 1, 100333-94-6; 2, 117469-71-3; 3, 117469-73-5; 3a, 117469-75-7; 4, 117469-74-6.

---

[7] Bianchini, C.; Meli, A.; Peruzzini, M.; Vizza, F.; Fujiwara, Y.; Jintoku, T.; Taniguchi, H. *J. Chem. Soc., Chem. Commun.* 1988, 299.

Stepwise Reaction of CS_2 with the Nickelacyclopentene Complexes $(\mathrm{R_3P})_2\overline{\mathrm{Ni}(\mathrm{CH_2CMe_2}\text{-}o\text{-}\mathrm{C_6H_4}})$. Influence of the Ancillary Phosphine Ligands

Juan Cámpora,[1a] Ernesto Carmona,*,[1a] Enrique Gutiérrez-Puebla,[1b] Manuel L. Poveda,[1a] and Caridad Ruiz[1b]

Departamento de Química Inorgánica e
Instituto de Ciencia de Materiales
Universidad de Sevilla-CSIC, Aptdo. 553
41071 Sevilla, Spain, and
Instituto de Química Inorgánica Elhúyar
y Departamento de Química Inorgánica
Universidad Complutense de Madrid-CSIC
28040 Madrid, Spain

Received August 10, 1988

Summary: The reaction of the nickelacyclopentene complexes $(\mathrm{R_3P})_2\overline{\mathrm{Ni}(\mathrm{CH_2CMe_2}\text{-}o\text{-}\mathrm{C_6H_4}})$ ($\mathrm{PR_3} = \mathrm{PMe_3}$, **1a**; $(\mathrm{R_3P})_2 = \mathrm{Me_2PCH_2CH_2PMe_2}$, dmpe, **1b**) with CS_2 follows a different course depending on the nature of phosphine coligands. Compound **1a** provides (3 equiv of CS_2, 20 °C) the known $\mathrm{Ni(C_2S_4PMe_3)PMe_3}$ (**2**) and the dithiolactone $\overline{\mathrm{S{=}C(S)CH_2CMe_2}\text{-}o\text{-}\mathrm{C_6H_4}}$ (**3**) through the intermediacy of the Ni(0) species $(\mathrm{Me_3P})_2\mathrm{Ni}(\overline{\mathrm{S{=}C(S)CH_2CMe_2}\text{-}o\text{-}\mathrm{C_6H_4}})$ (**4a**) which contains **3** as an η^2-C═S ligand and can be isolated from **1a** and CS_2 (1 equiv, −90 °C). Complex **1b** reacts with CS_2 to provide first a 1,1-dithiolate derivative, $(\mathrm{dmpe})\overline{\mathrm{Ni}(\mathrm{SSCCH_2CMe_2}\text{-}o\text{-}\mathrm{C_6H_4}})$ (**5**), and then the trithiocarbonate $(\mathrm{dmpe})\overline{\mathrm{Ni}(\mathrm{S_2}}\mathrm{CS})$ (**6**) along with the thioketone $\overline{\mathrm{S{=}CCH_2CMe_2}\text{-}o\text{-}\mathrm{C_6H_4}}$ (**7**). These two reactions can be respectively thought of as the insertion of CS_2 into both Ni–C bonds of **1b** and as the reductive disproportionation of two molecules of CS_2. In the latter process, the thiocarbonyl group becomes incorporated into the thioketone functionality of **7**.

The reactivity of transition-metal complexes toward small, unsaturated molecules continues to arouse much attention.[2] We have recently shown that the nickelacyclopentene complex $(\mathrm{Me_3P})_2\overline{\mathrm{Ni}(\mathrm{CH_2CMe_2}\text{-}o\text{-}\mathrm{C_6H_4}})$ (**1a**) reacts with unsaturated C1 molecules such as CO, CO_2, and CH_2O, with formation of products resulting from insertion of the unsaturated molecule into either the nickel alkyl or the nickel aryl carbon bonds.[3] Only in the case of CO does reductive elimination (to Ni(0) and the corresponding ketone) follow insertion. In this paper we wish to present additional studies concerning the related reactions of **1a** and its dmpe analogue **1b**, $(\mathrm{dmpe})\overline{\mathrm{Ni}(\mathrm{CH_2CMe_2}\text{-}o\text{-}\mathrm{C_6H_4}})$ (dmpe = $\mathrm{Me_2PCH_2CH_2PMe_2}$), with CS_2. As shown in Scheme I, these correspond to a novel type of reactivity and have led to a variety of organic and inorganic species.[4]

---

[1] (a) Universidad de Sevilla. (b) Universidad Complutense de Madrid.

[2] See, for example: Collman, J. P.; Hegedus, L. S.; Norton, J. R.; Finke, R. G. *Principles and Applications of Organotransition Metal Chemistry*; University Science Books: Mill Valley, CA, 1987.

[3] Carmona, E.; Palma, P.; Paneque, M.; Poveda, M. L.; Gutiérrez-Puebla, E.; Monge, A. *J. Am. Chem. Soc.* 1986, *108*, 6424.

[4] Satisfactory analytical data (C, H, S; Pascher, Bonn and Analytical Service, University of Sevilla) have been obtained for all new compounds (see Table IV, supplementary material).